



Plasticity 2020 – Cancun

Modelling the Influence of Plastic Deformation on Local Material Stiffness to Predict the Crack Growth Behaviour of a Nickel Based Superalloy

W. Lavie, B. Engel, J. P. Rouse and C. J. Hyde

University of Nottingham

Background

At present 3 Gtonnes of CO₂ are produced every year by air travel. This is completely unsustainable and is driving the need for greater efficiency in aeroengines.

Similar motivations are present in the power generation sector.

Future engineering systems are expected to utilise higher temperatures and lower component weights in order to meet targets.

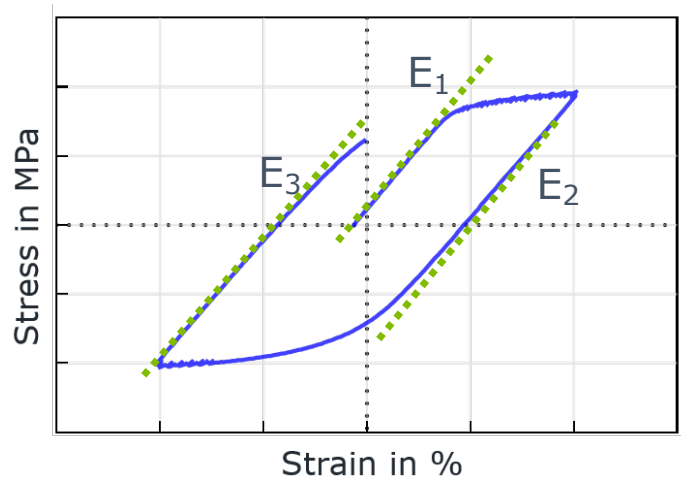
Much work is being carried out at UoN to increase service life of present and future critical components and reduce CO₂ emissions, by enabling more accurate predictions of design life and in-service behaviour.

Better understanding of the properties of the materials that drive the behaviour of them in service, along with modelling capabilities to represent this will lead to technological leaps.

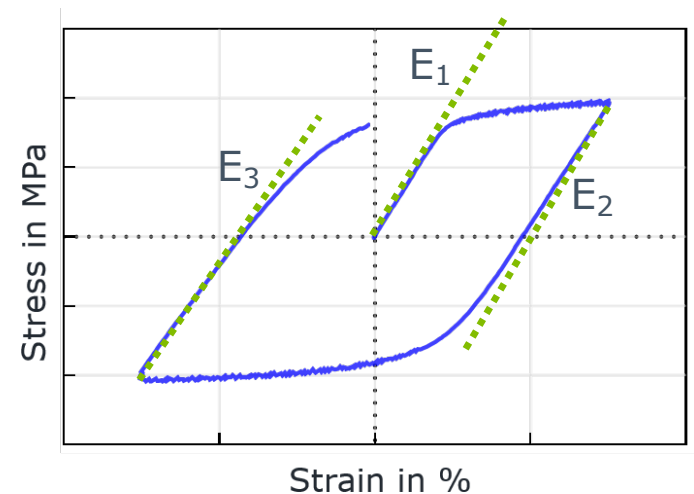


Introduction

During LCF experimental testing of a Nickel-based superalloy, it was noticed that there was a cyclic decrease in Young's Modulus.



- $\varepsilon_{a,t} = 1 \%$, $R = -1$ & 700°C
- Decreasing Young's moduli: $E_1 > E_2 > E_3$
- $E_3 = 0.9E_1$
- After stabilisation, $E_{\text{stab}} = 0.87E_1$



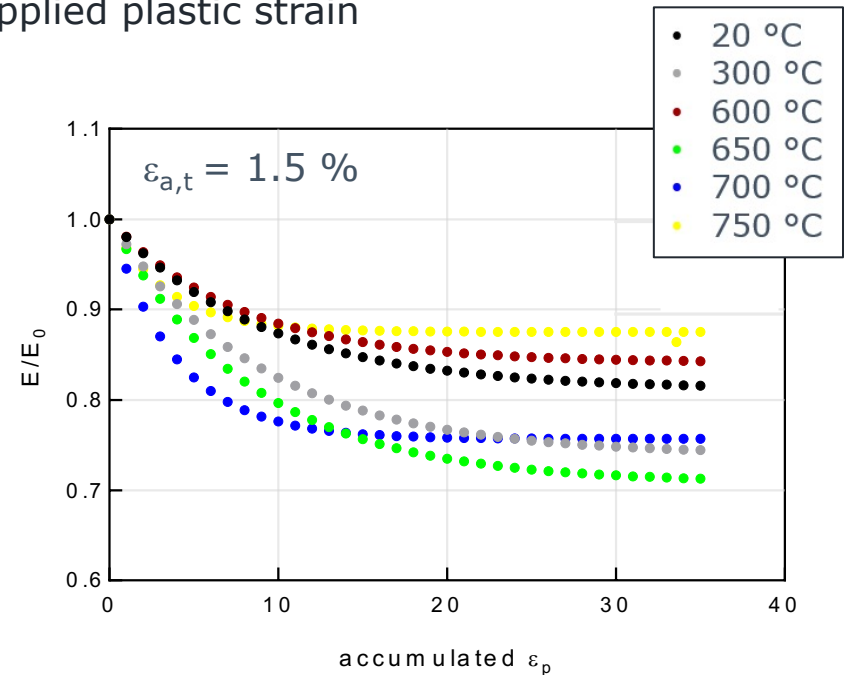
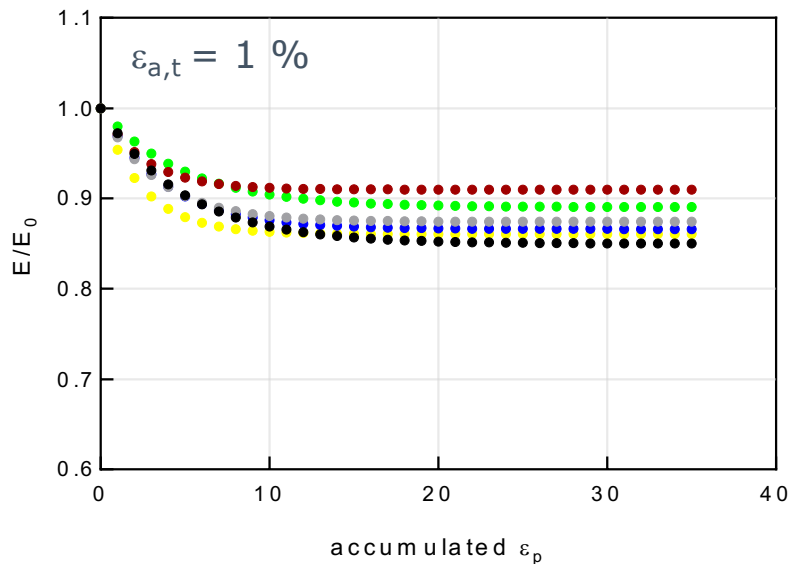
- $\varepsilon_{a,t} = 1.5 \%$, $R = -1$ & 700°C
- Decreasing Young's moduli: $E_1 > E_2 > E_3$
- $E_3 = 0.85E_1$
- After stabilisation, $E_{\text{stab}} = 0.75E_1$

Observation

For tests with no induced plasticity ($\varepsilon_{a,p} \approx 0$), no measurable change in Young's modulus was observed.

Therefore, plasticity induced changes in elastic properties are present

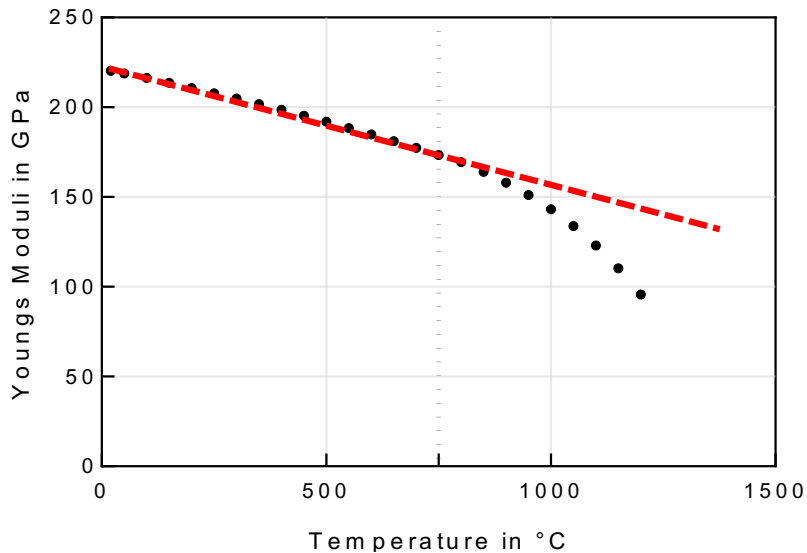
Decrease of Young's moduli is dependent on applied plastic strain



Characterisation

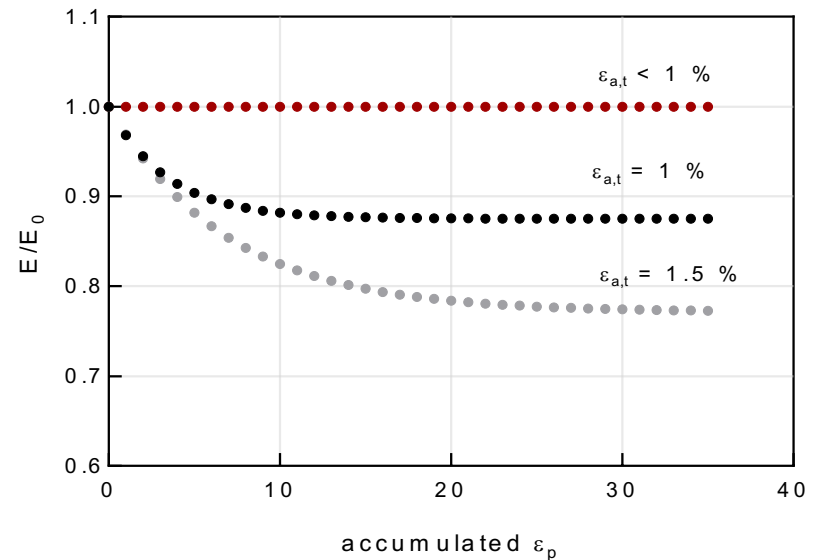
- Step 1: Calculation of the initial Young's modulus E_0 As a function of temperature (from tensile testing).
 - Up to 750 °C a linear behaviour can be assumed:

$$E_0 = a \cdot T + b$$



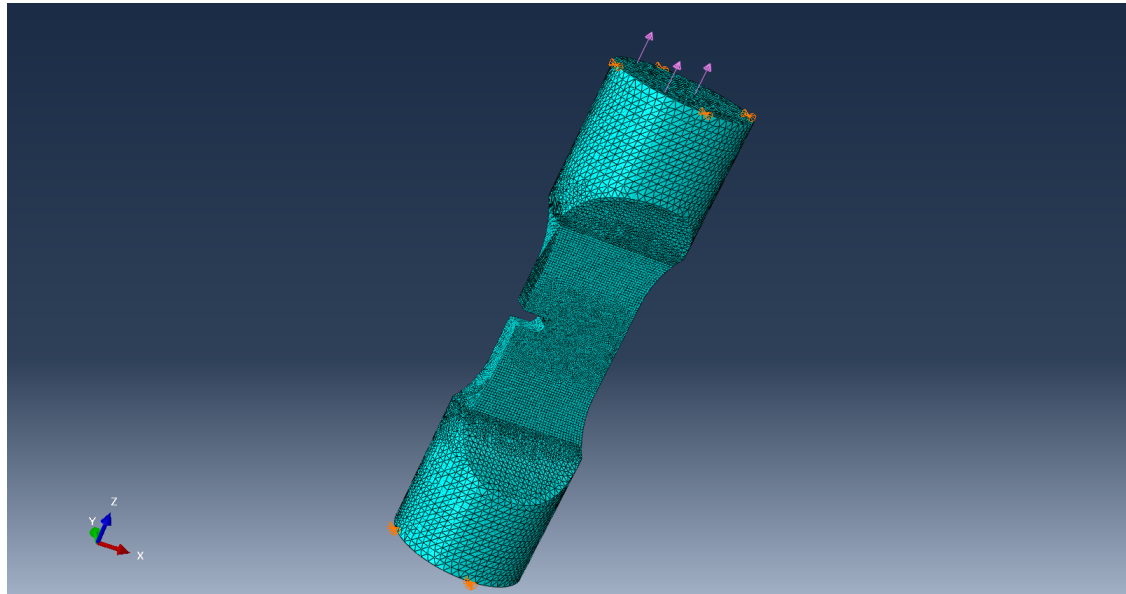
- Step 2: Determination of a function to represent the decrease in Young's modulus as a function of accumulated plastic strain:

$$E = 1 - (c \cdot (1 - \exp(-d \cdot \varepsilon_p))) \cdot E_0$$



Aim

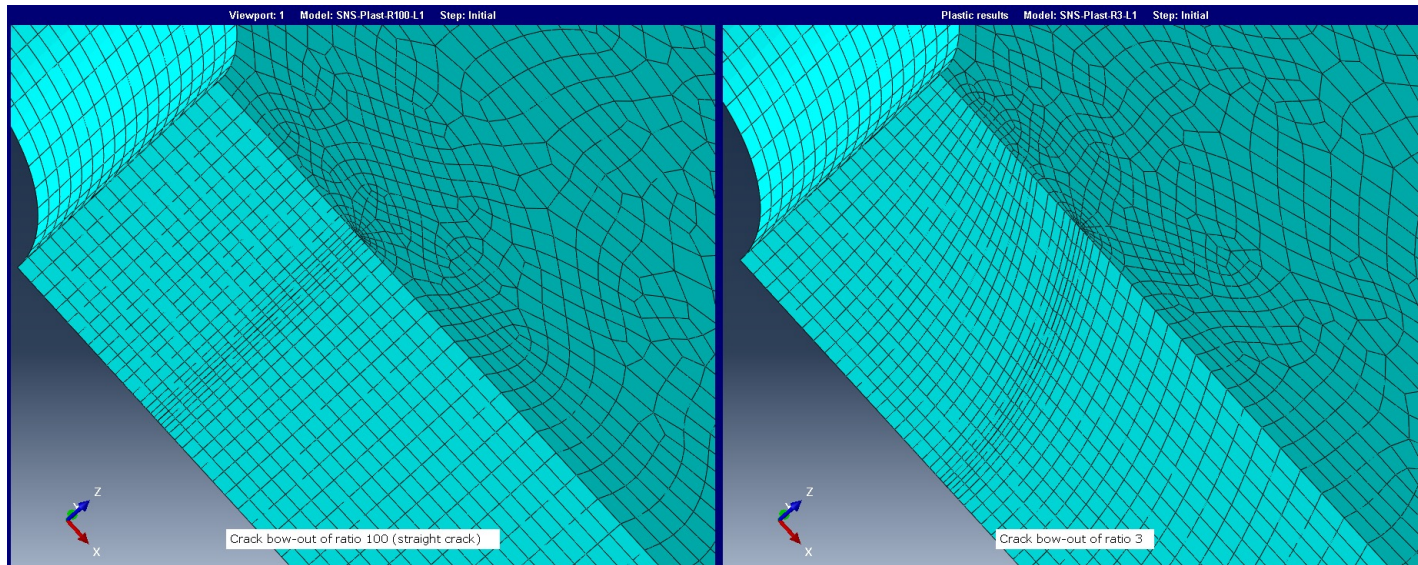
Model the effect of the experimentally observed plasticity-induced changes in elastic properties on crack growth behaviour (through the lens of SIF).



SEN specimen considered for the study

Methodology

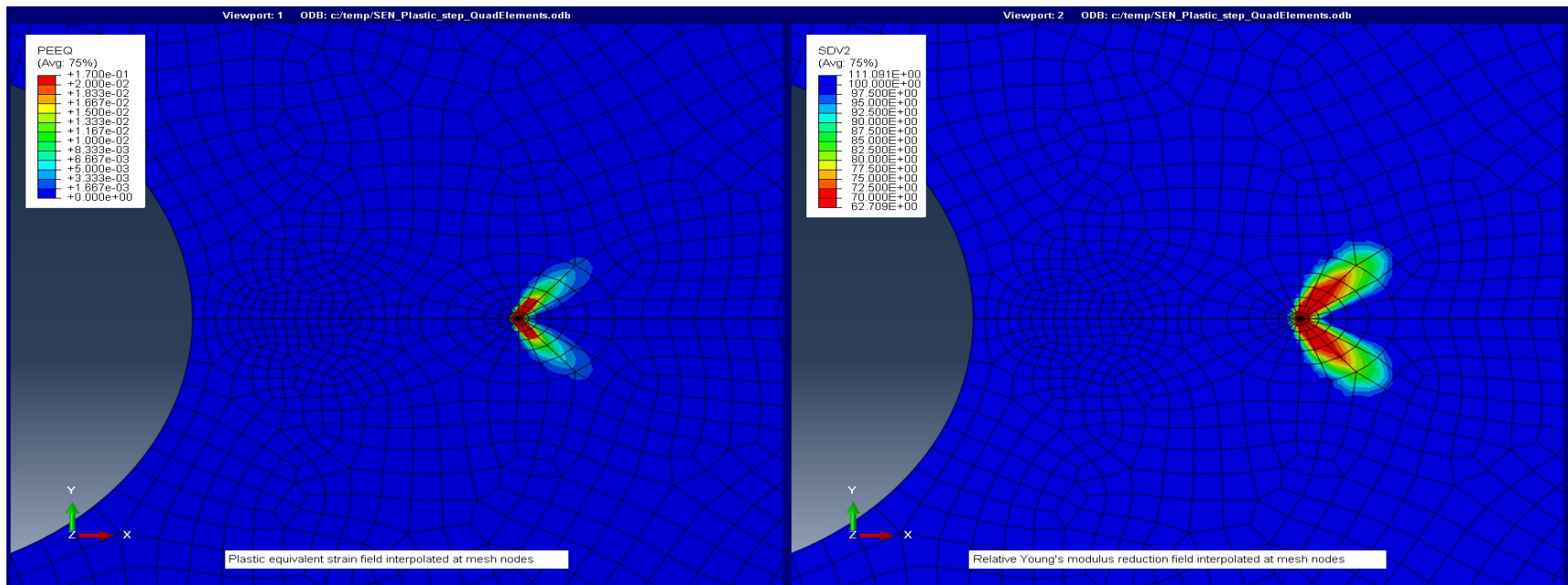
- Abaqus FEM simulation
- Two-step sequential simulation:
 1. Plastic model to extract plastic strain
 2. Elastic model (with modified Young's modulus field as a function of local plastic strain) to extract SIF using contour integral method
- Cracks of different (tunnelling) geometries have been modelled



Procedure

1st Step: Plastic analysis

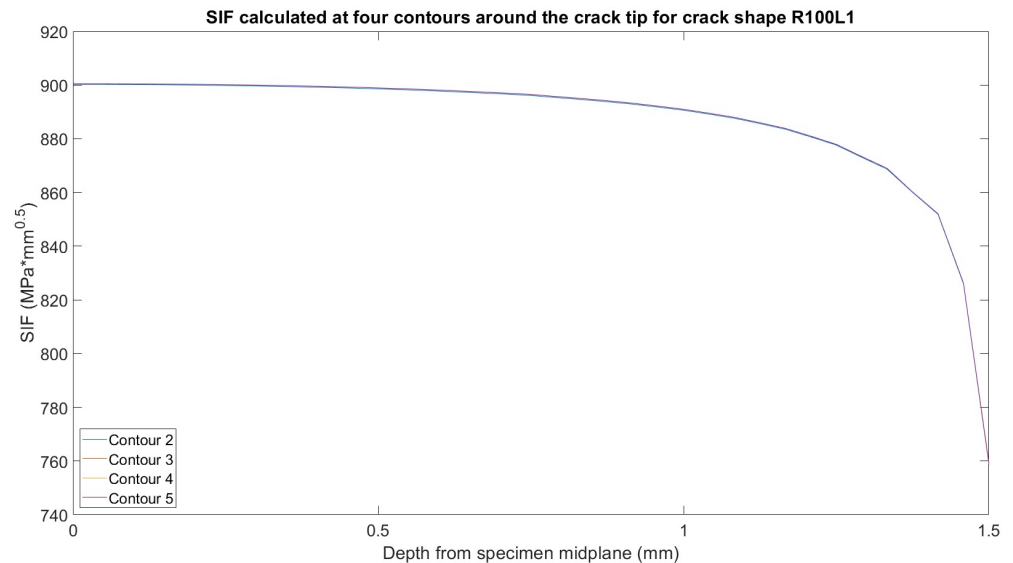
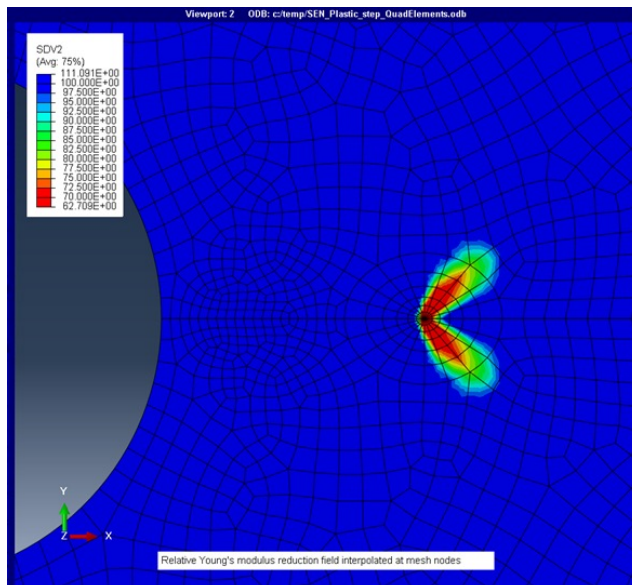
- Plastic model at the neighbourhood of the crack
- Subroutine USDFLD used to evaluate the Young's Modulus as a function of PEEQ



Procedure

2nd Step: Elastic analysis

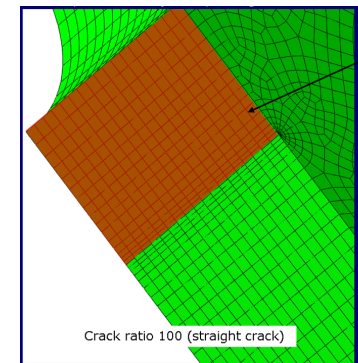
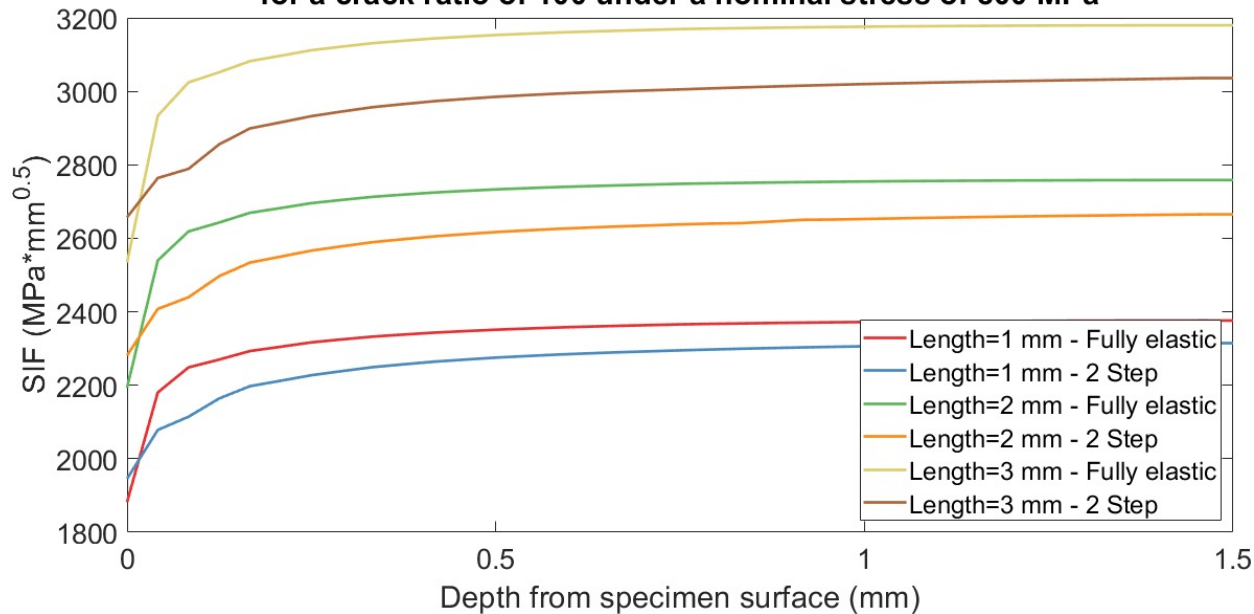
- Elastic model with varying E at crack neighbourhood
- E reduction field obtained from plastic step
- SIF calculated through contour integrals



Results

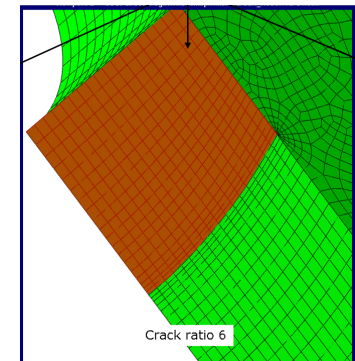
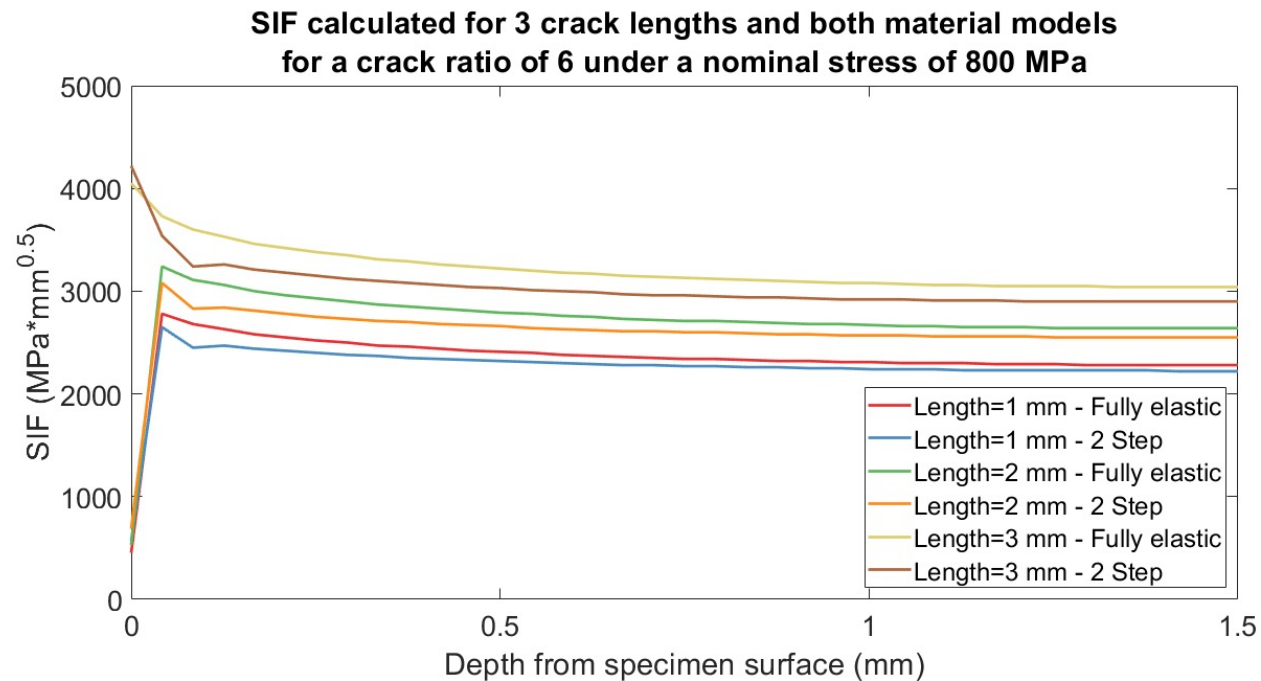
800 MPa for 1 mm pre-crack, straight crack

SIF calculated for 3 crack lengths and both material models
for a crack ratio of 100 under a nominal stress of 800 MPa



Results

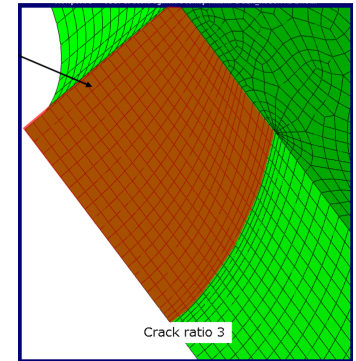
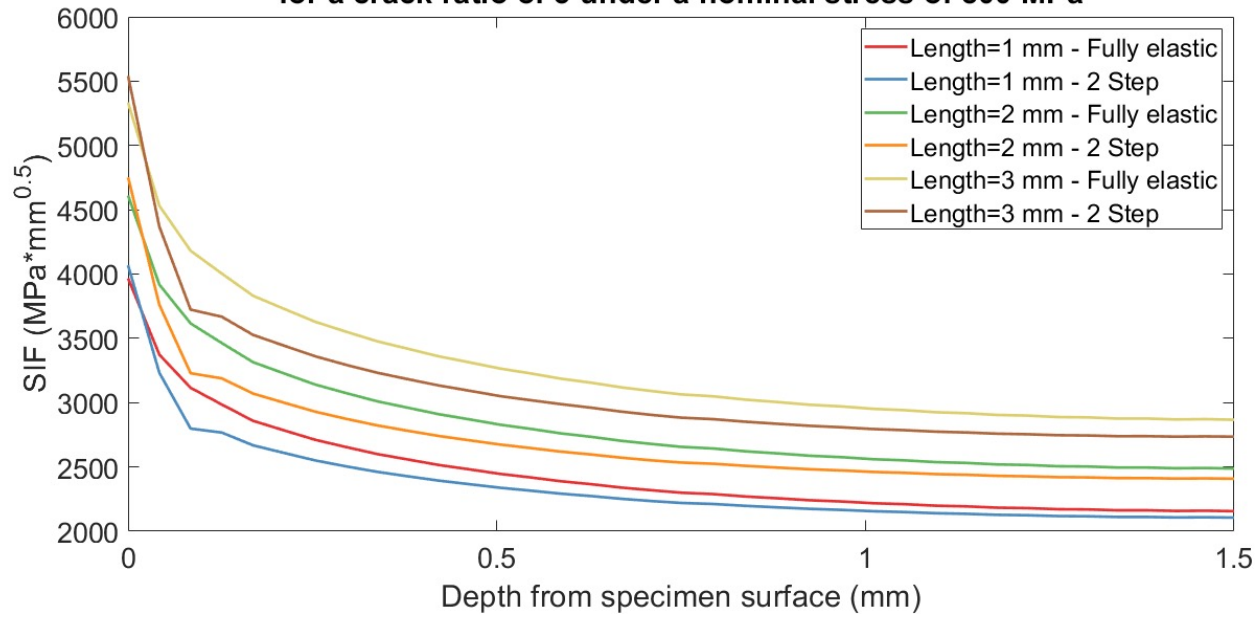
800 MPa for 1 mm pre-crack, low tunnelled crack



Results

800 MPa for 1 mm pre-crack, high tunnelled crack

SIF calculated for 3 crack lengths and both material models
for a crack ratio of 3 under a nominal stress of 800 MPa



Conclusions

- During LCF experimental testing of a Nickel-based superalloy, it was noticed that there was a cyclic decrease in Young's Modulus.
- For tests with no induced plasticity, this change in Young's modulus was not observed. Therefore, plasticity induced changes in elastic properties are present and are a function of applied plastic strain.
- This has been applied to SEN FE simulations via a plastic strain dependant Young's modulus field in the specimen geometry.
- Even for relatively small decreases in Young's modulus, effects are consistently observed on the stress intensity factor at the crack tip.
- Relative impact of the decrease seems to be tied to the shape of the crack
 - The flatter the crack the higher the observed difference (load shedding)

Further developments

- Microstructural determination of the cause of this apparent decrease in Young's modulus (thought to be the pinning and subsequent bowing of dislocations during plasticity).
- Comparison of FE calculated SIFs for SEN geometries to be compared with experimental results.



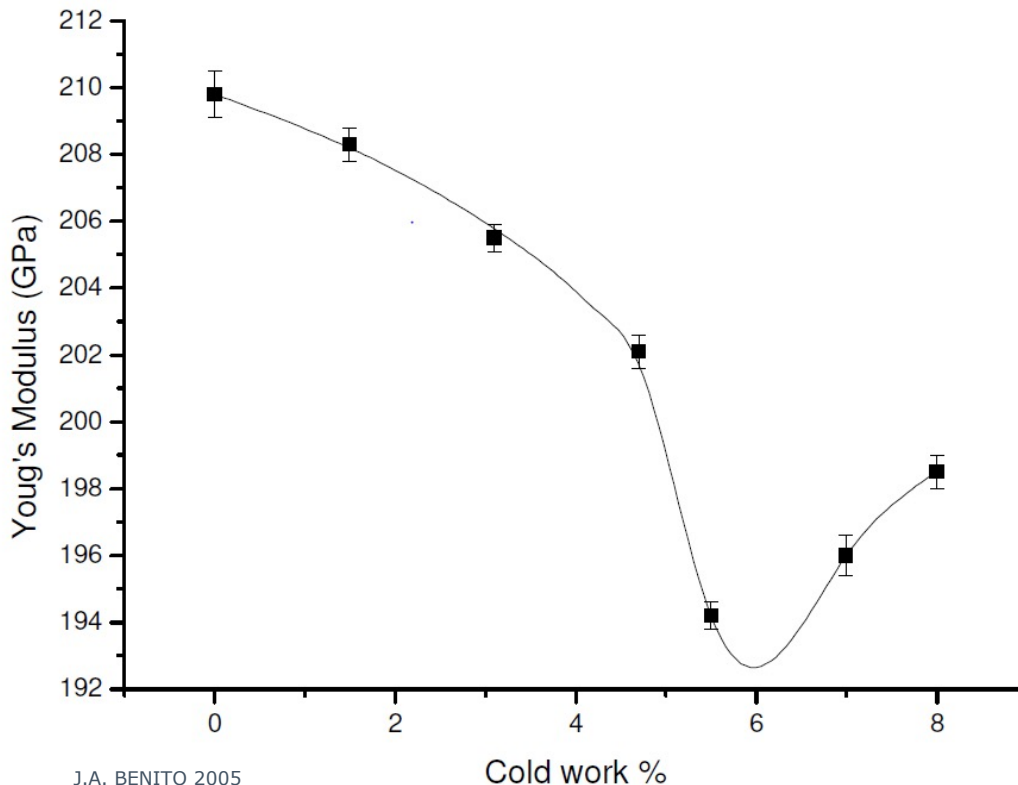
Thank You for Your Attention.
Any Questions?

Literature Review – Changes in Young's Moduli

- Changes in Young's Moduli in dependence of plastic strains up to 15 % are known for:
 - Pure iron, low carbon steels, stainless steel, aluminium, brass, copper, stainless steel
 - At room temperature and very high plastic strains in tension tests (no cyclic testing)
 - Effects are mostly attributed to dislocation distribution (no effect of texture, residual stresses)

DevTMF

Where does the decrease come from? – Literature Review



$$\frac{\Delta E}{E} = -\rho \cdot \frac{l^2}{6 \cdot \alpha}$$

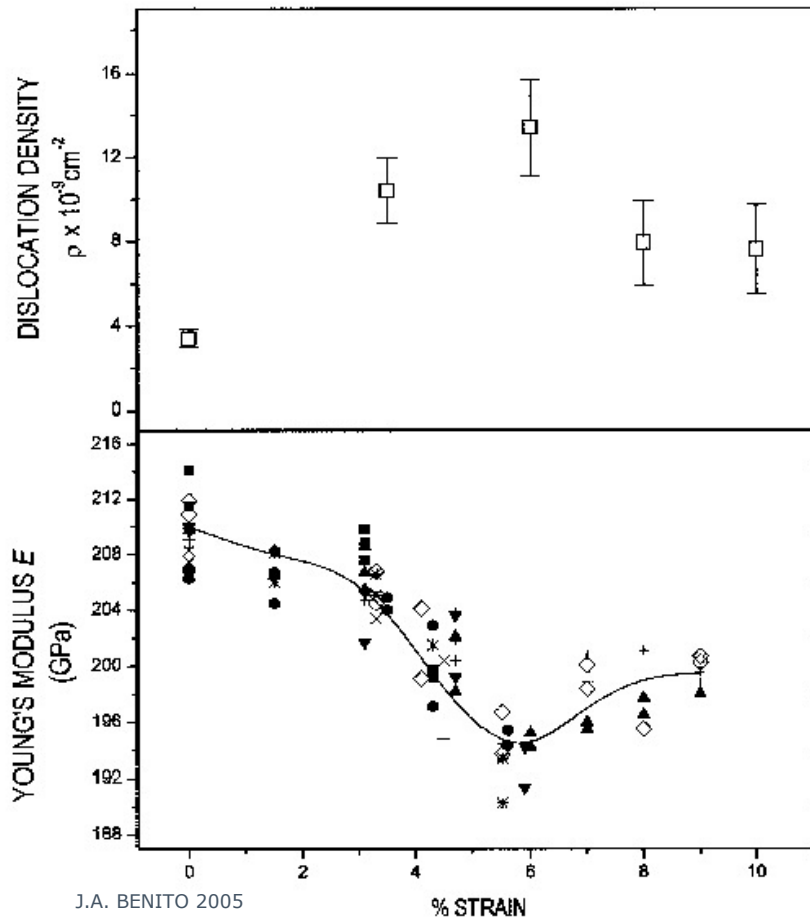
ρ : dislocation density

l : is the average length
line of dislocations between
pinning points

α : is a function of l

DevTMF

Pure Iron in tensile test



J.A. BENITO 2005

Their conclusion:

Increase of plastic strain leads to increase in dislocation density

Dislocation form a bow out while formation of cellular arrays, which gives additional strain → decreases Young's Moduli

Recovery attributed to no new formation of cellular dislocation distribution

Benchmarking Abaqus results

- Comparison to 2D formulas from the literature
 - Jintegral : Bucci et al. 1972
 - SIF: Evans et al. 2014
- Comparison to 3D formulas from the literature
 - SIF : Newmann, Raju 1984

Benchmarking : Bucci et al. 1972

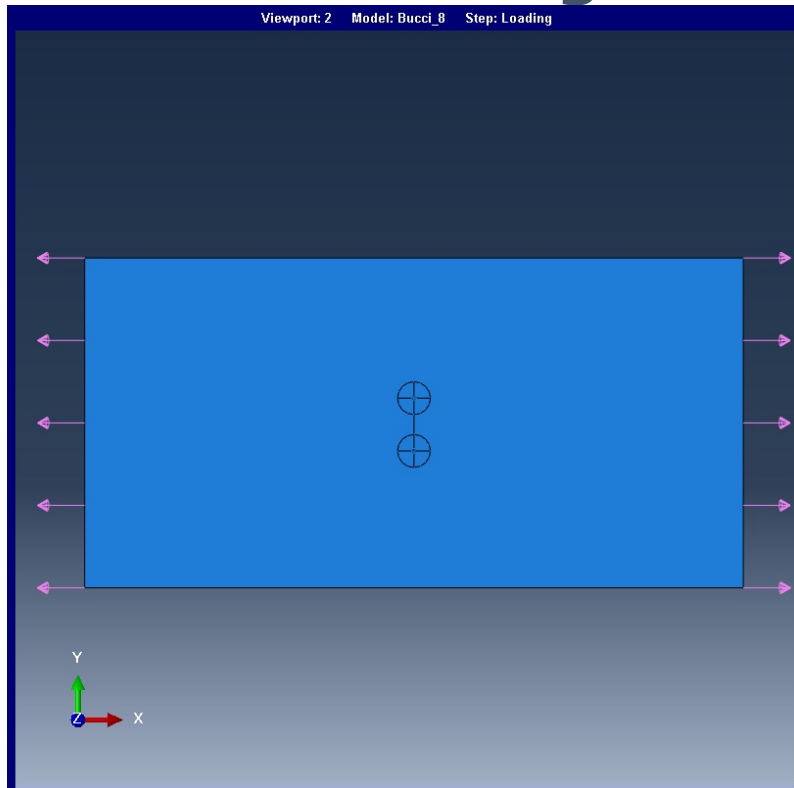


Figure 3 : Geometry considered by Bucci et al.

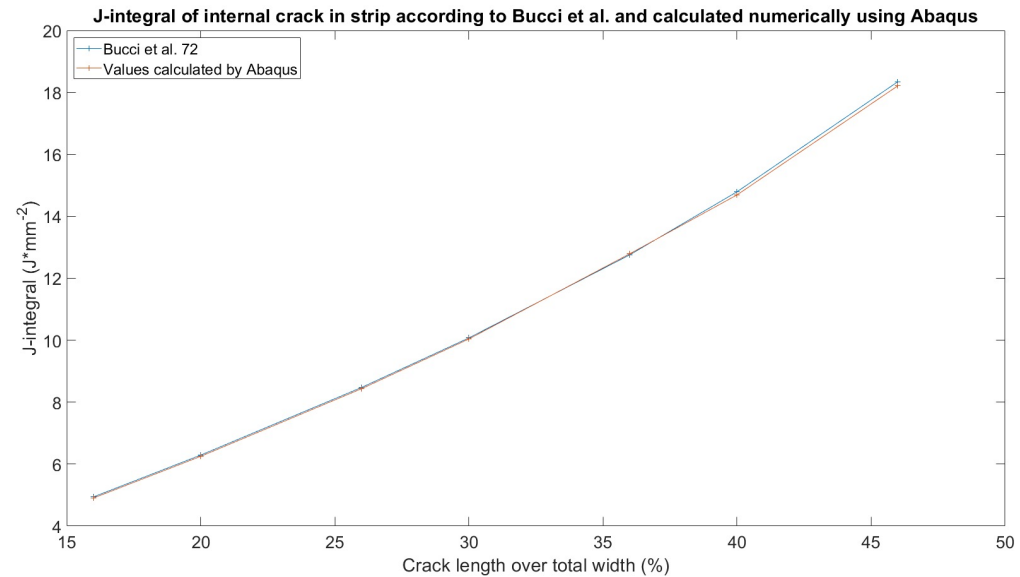


Figure 4 : Results computed with the Bucci formula and by Abaqus

Benchmarking : Evans et al. 2014

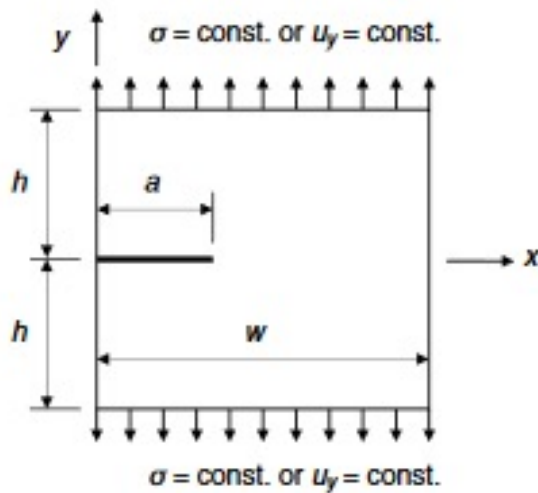


Figure 5 : Geometry considered by Evans et al.

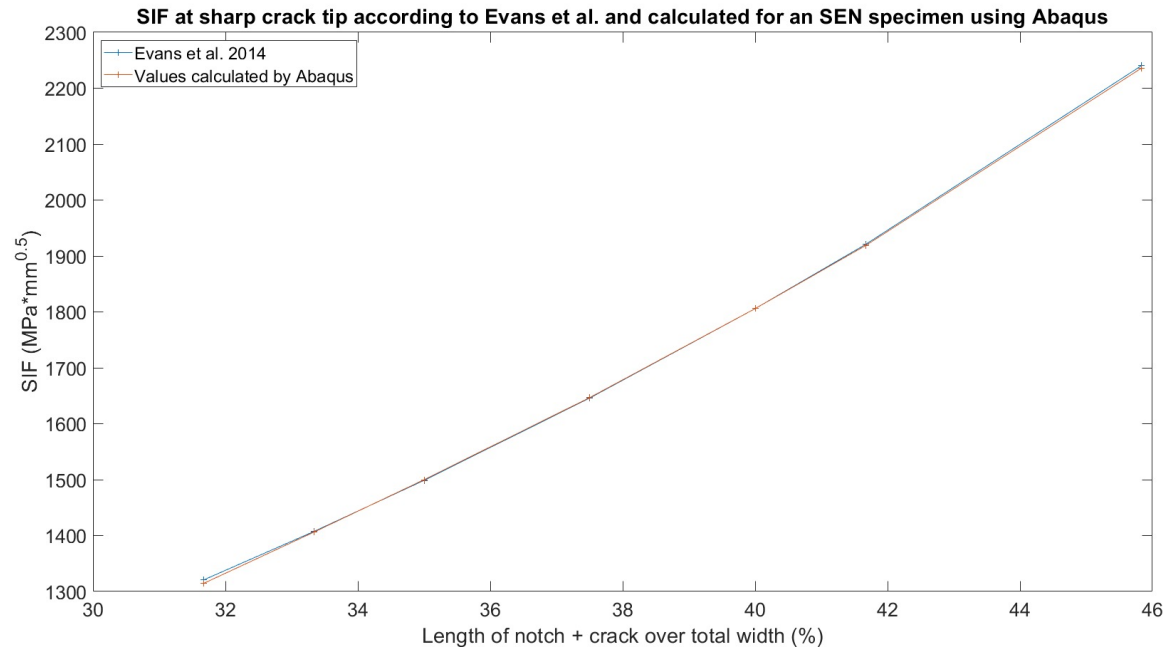
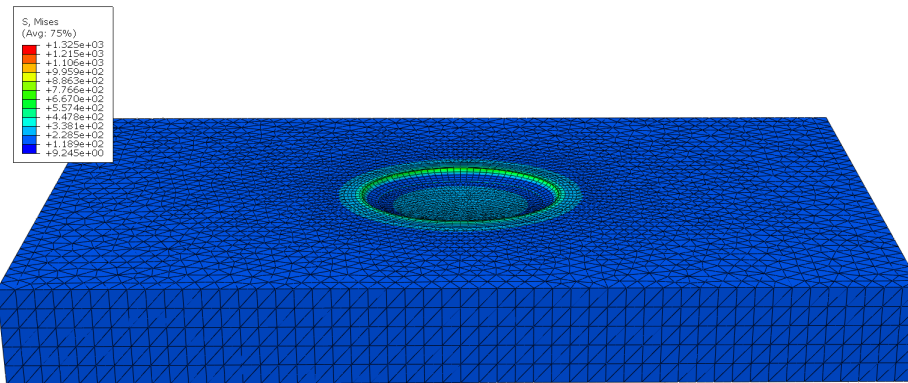


Figure 6 : Results computed with the Evans formula and by Abaqus

Benchmarking : Newman and Raju 1972



NEWMAN and RAJU

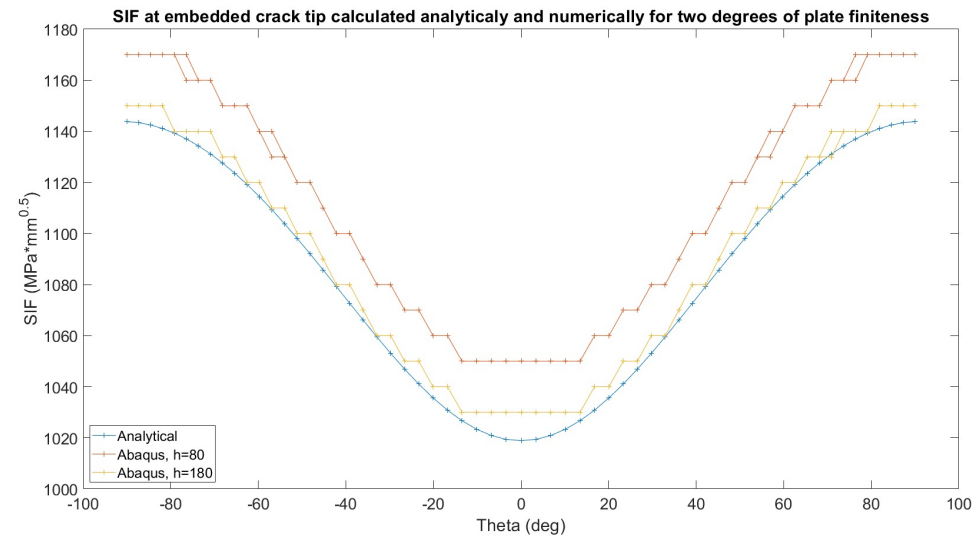


Figure 8 : Results computed with the Newman-Raju formula and by Abaqus

Simplifications

- Exploiting planes of symmetry

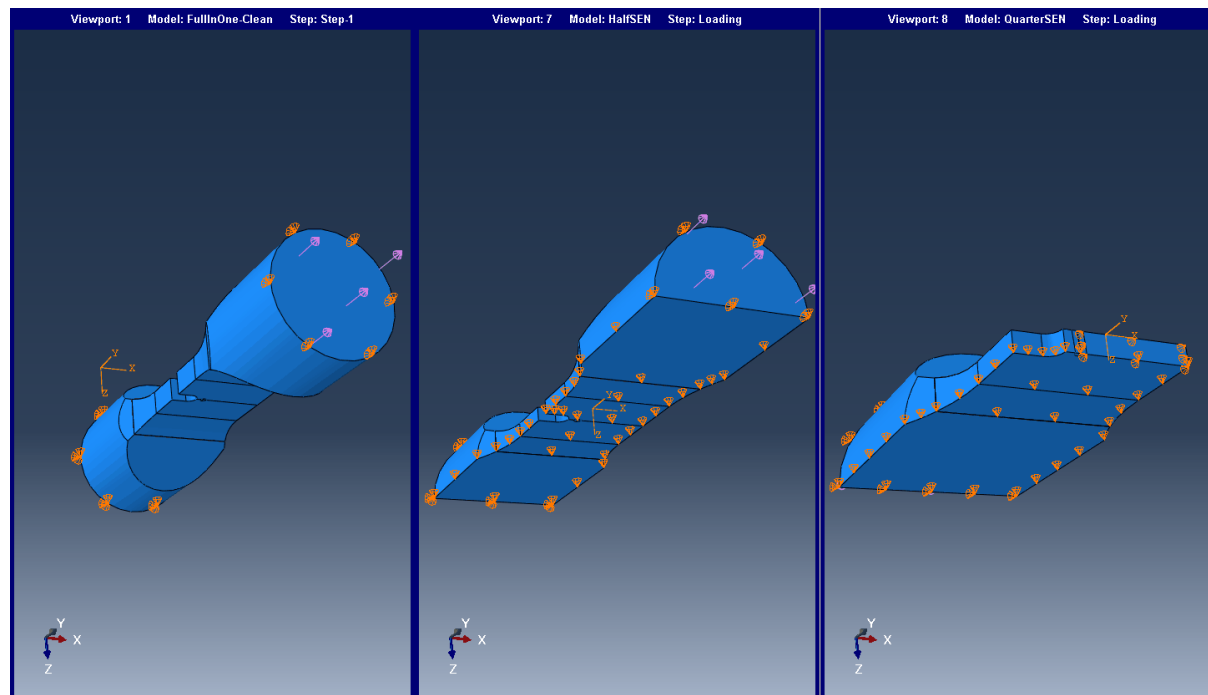


Figure 9 : Three models exploiting various symmetry planes

Simplifications : exploiting planes of symmetry

- Comparing SIF for all three models

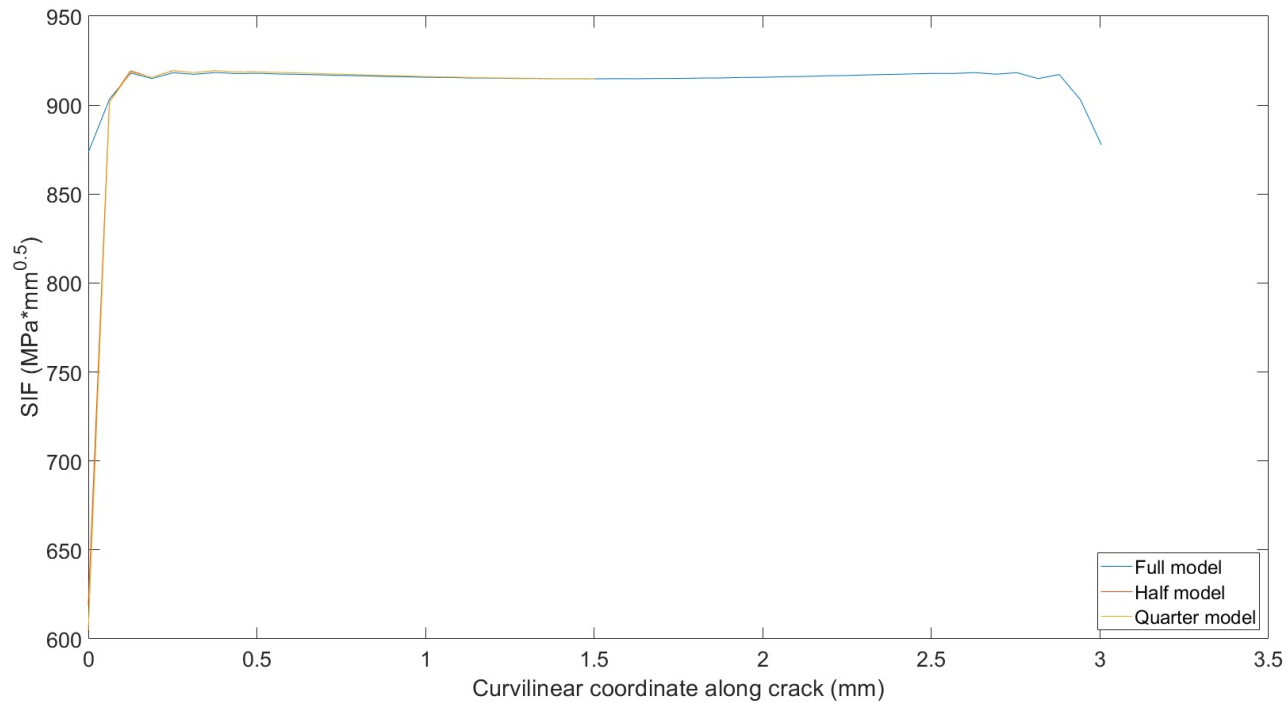


Figure 10 : SIF calculated for the three models

Simplifications : Exploiting planes of symmetry

- Comparing maximum von Mises equivalent stress

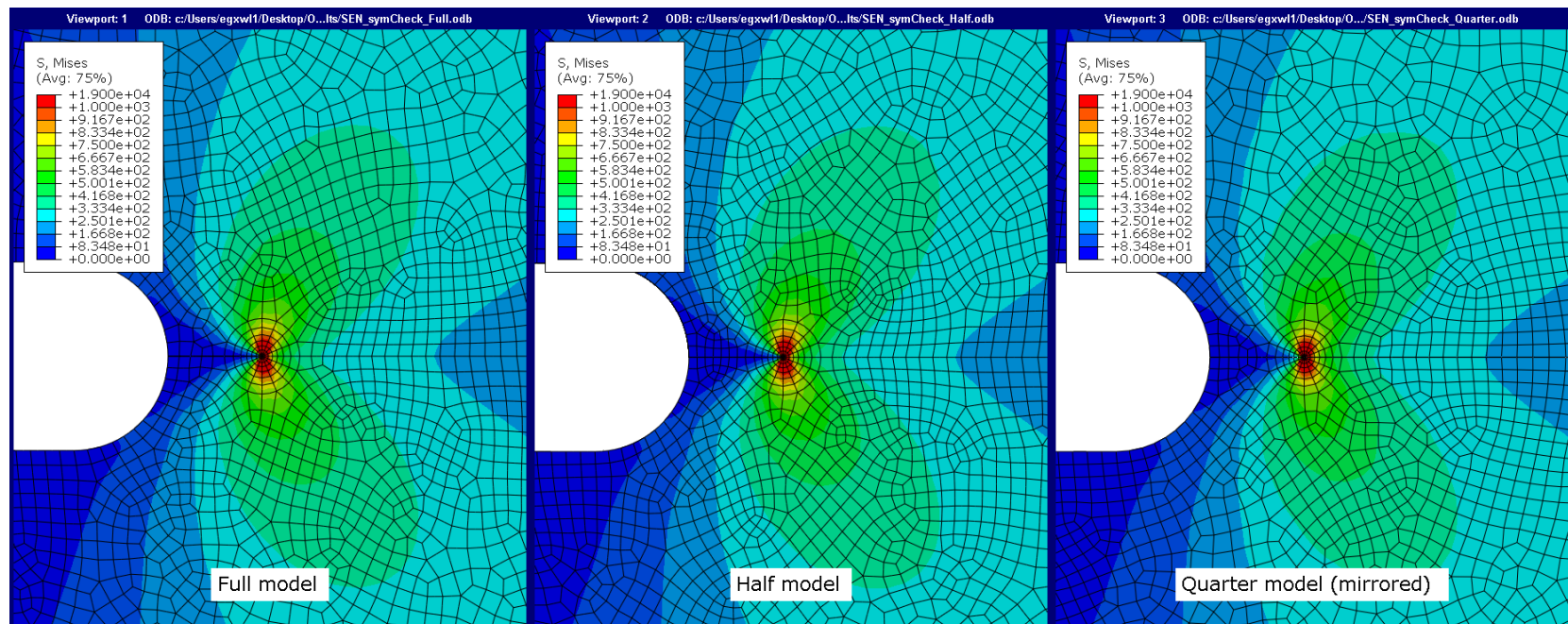


Figure 11 : Max. principal stress calculated for the three models

Simplifications

- Ignoring geometric non-linearity

SIF calculated for sharp bowed crack in a SEN specimen taking into account and not taking into account non-linear geometry effects

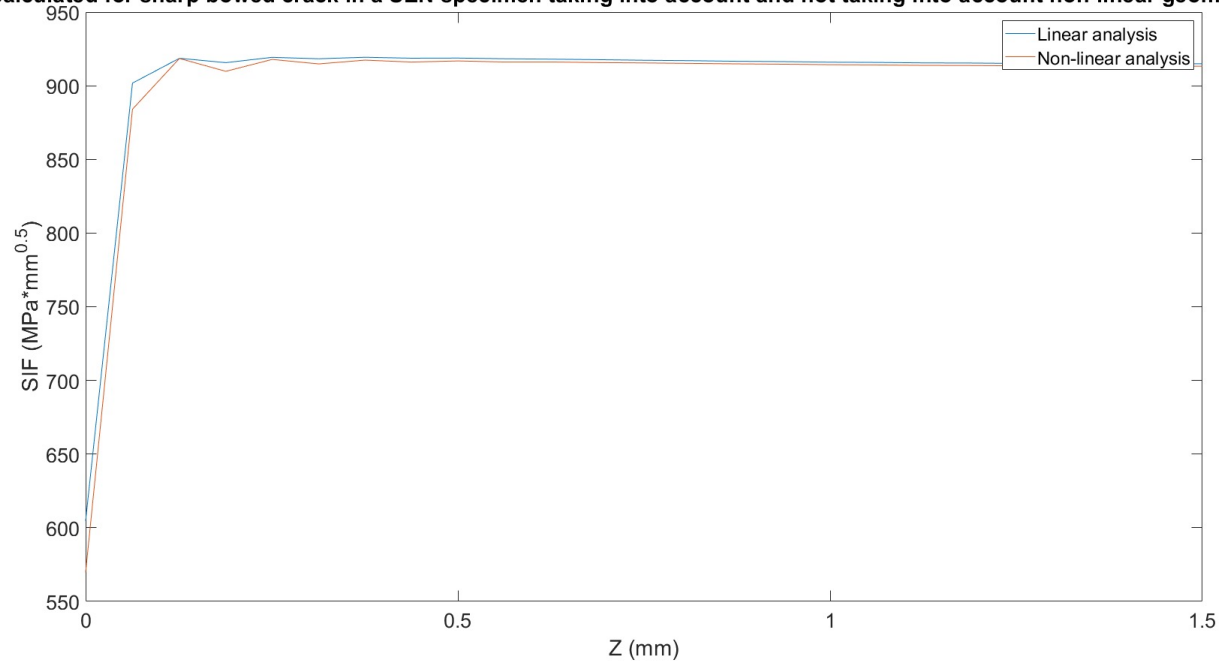


Figure 12 : SIF calculated with and without considering geometric non-linearity

Mesh convergence

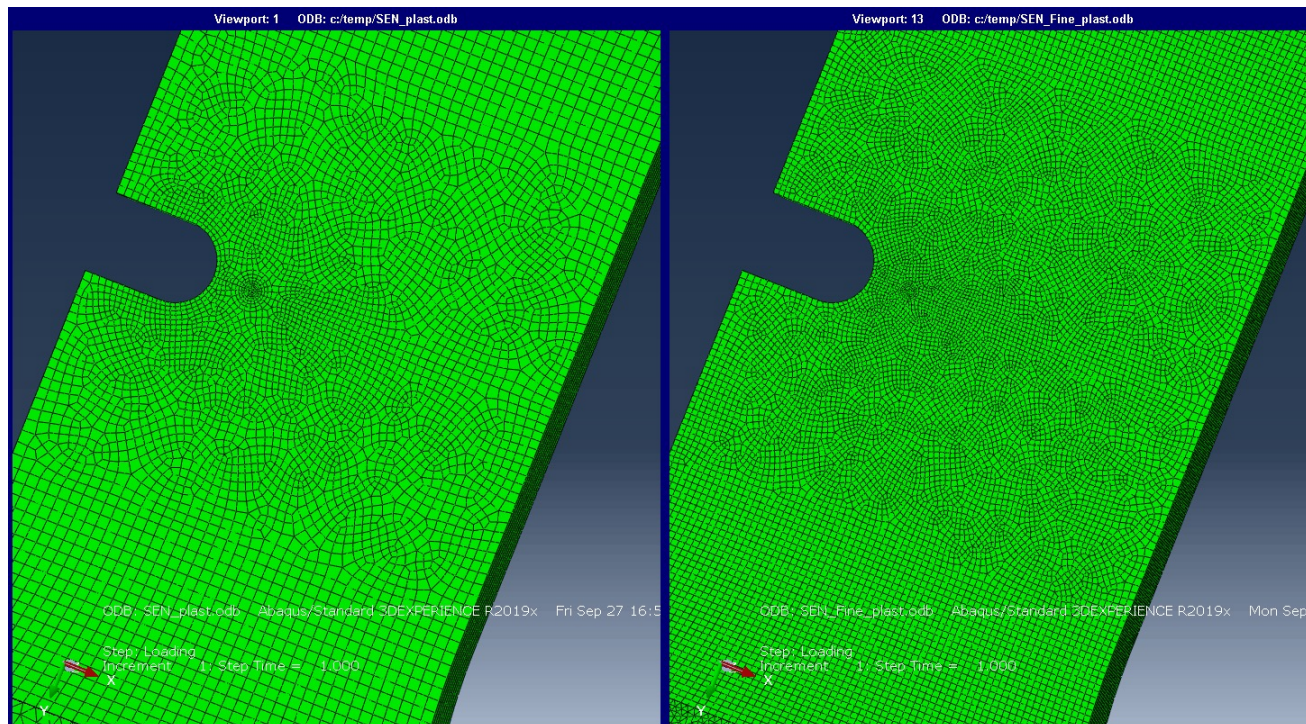


Figure 13 : A coarse and a fine mesh

Mesh convergence : convergence of the SIF

- Coarse meshes are sufficient when considering SIF

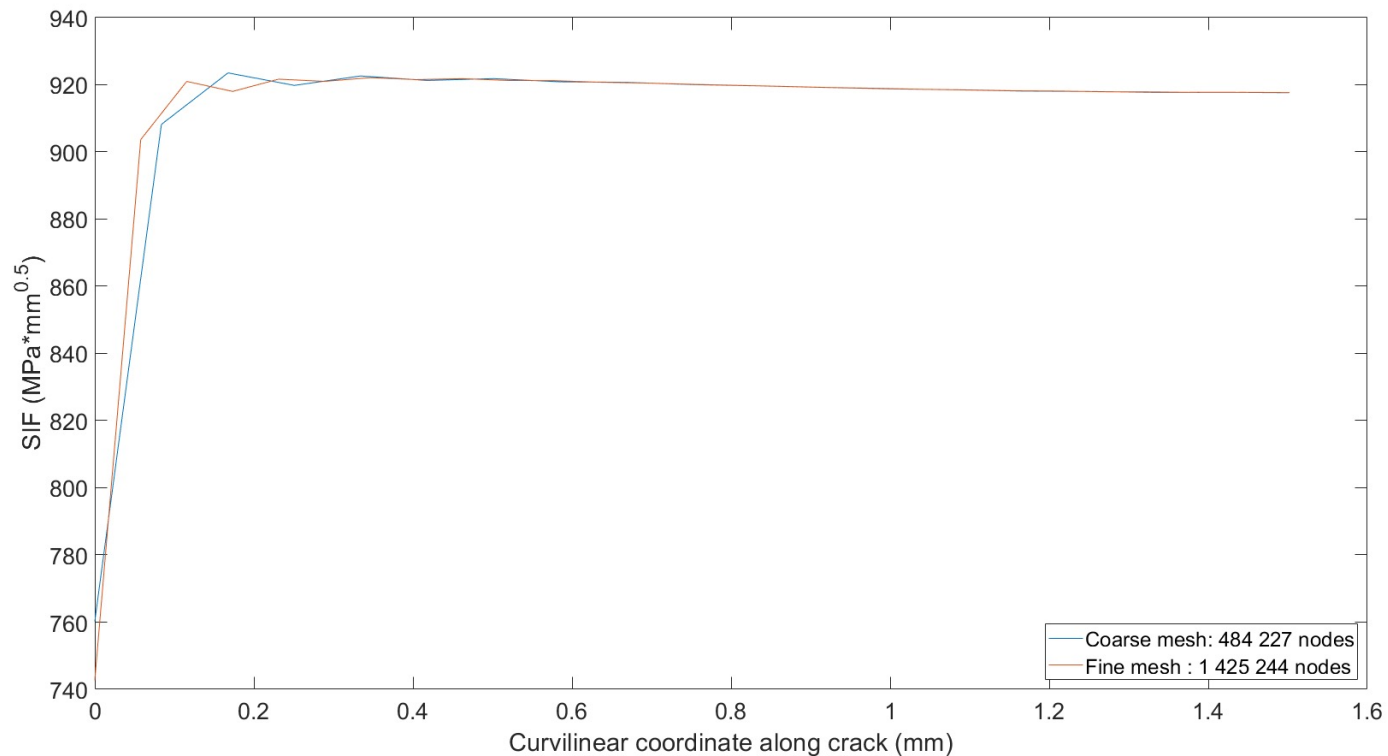
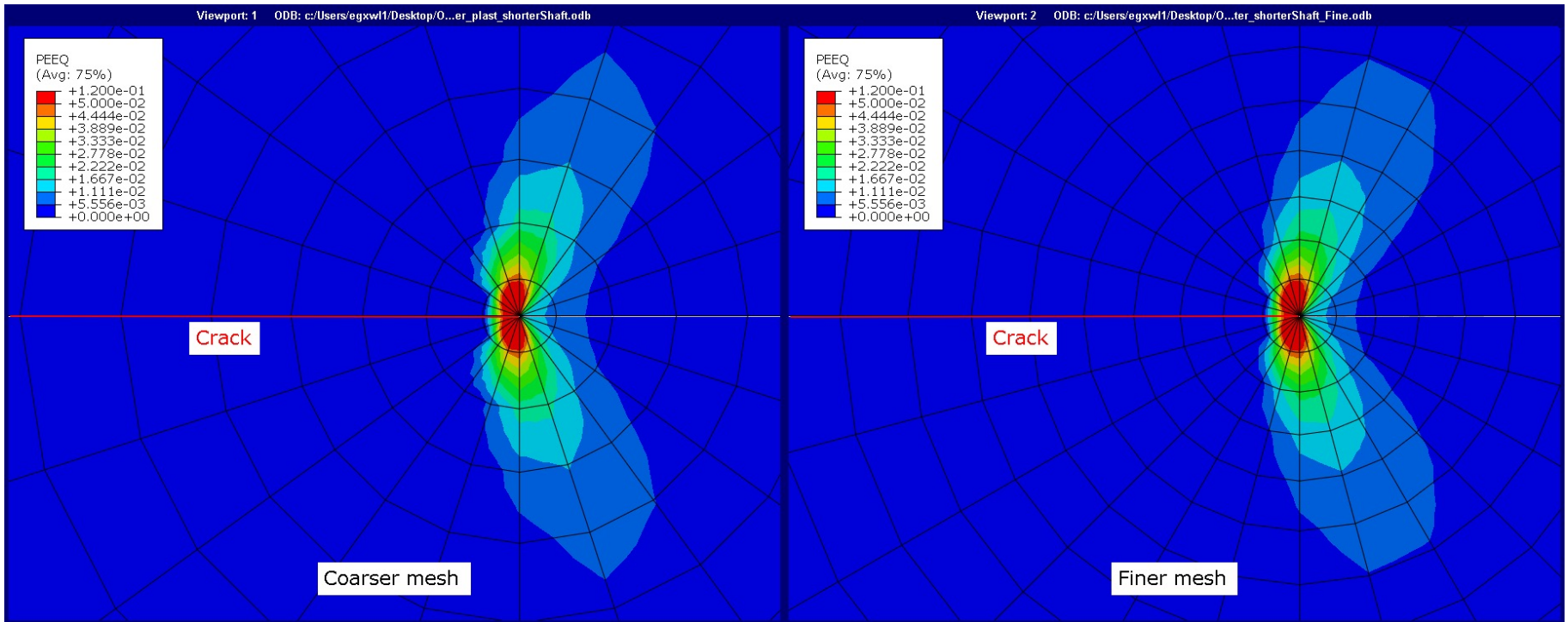


Figure 14 : SIF calculated for two degrees of mesh refinement

strain



Mesh convergence : comparing average normalised plastic strain error indicators

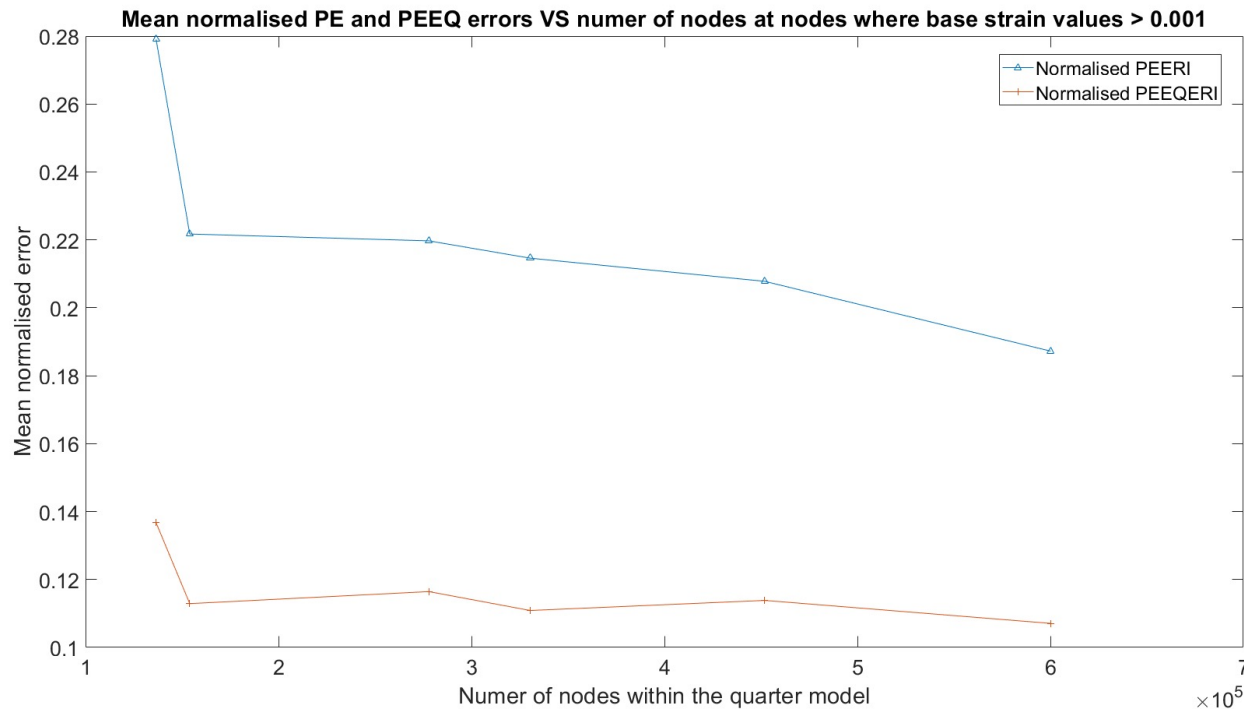
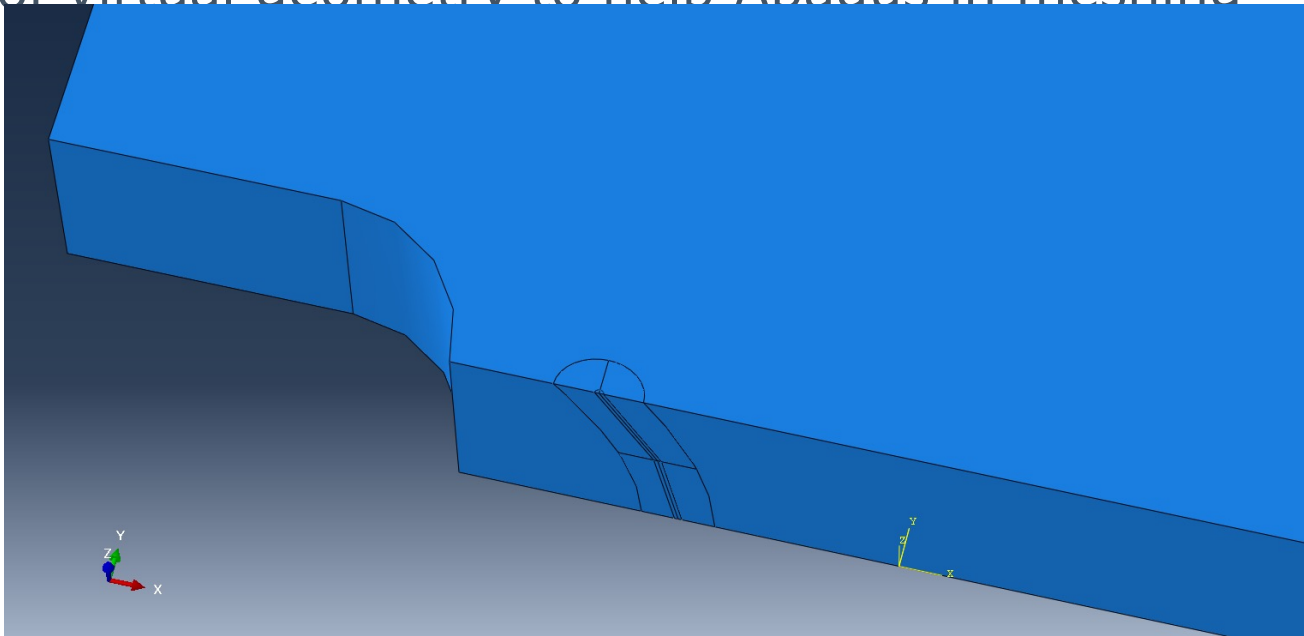


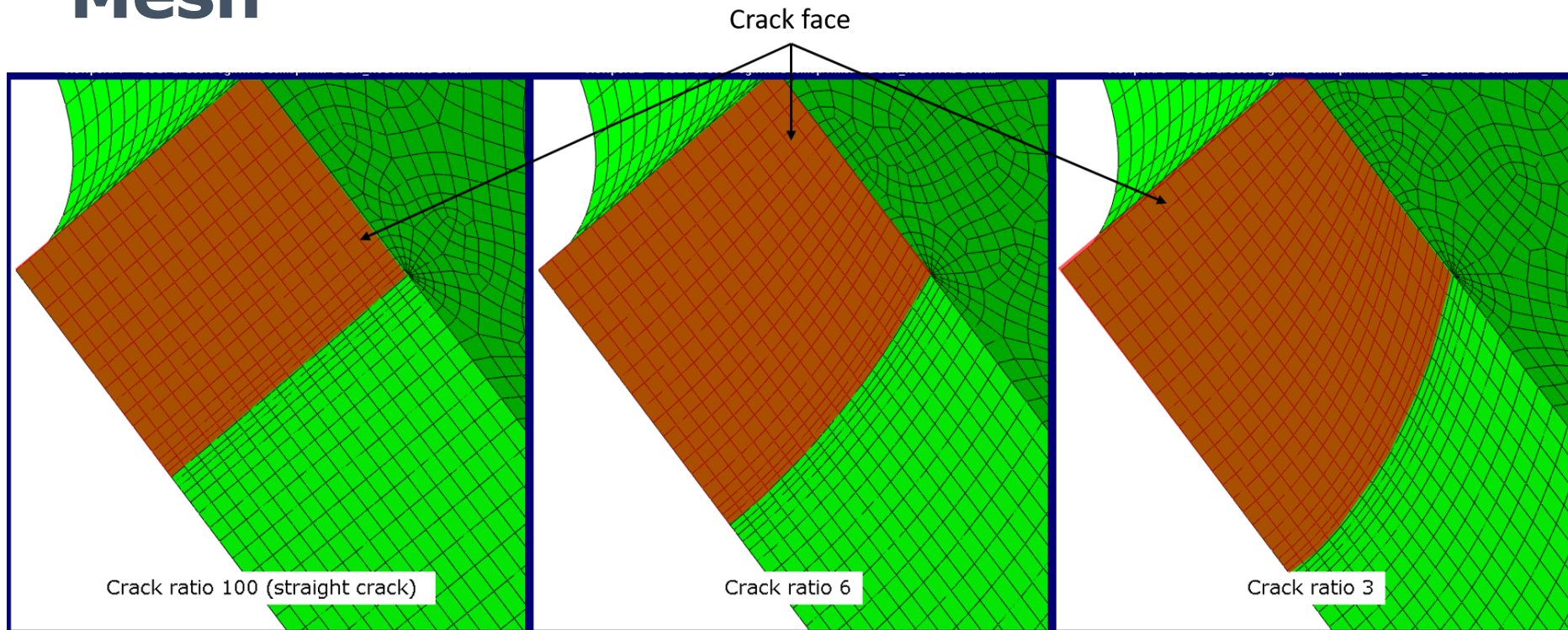
Figure 16 : Mean normalised plastic strain errors according to Abaqus

Geometry

- Classic SEN specimen
- Quarter model
- Use of virtual geometry to help Abaqus in meshing



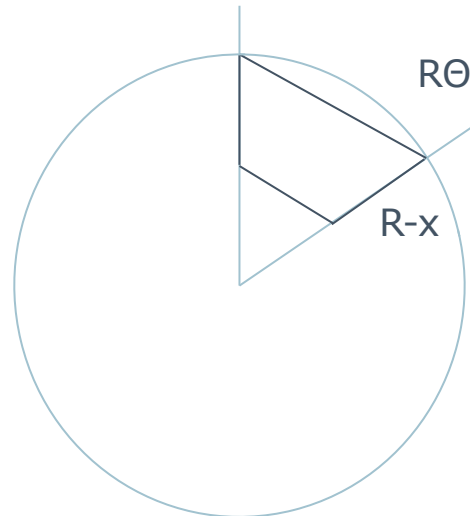
Mesh



Inherent meshing difficulties

- Contour integrals necessitate concentric element rings
- Many elements in a ring lead to heavily biased elements

→ Trade-off

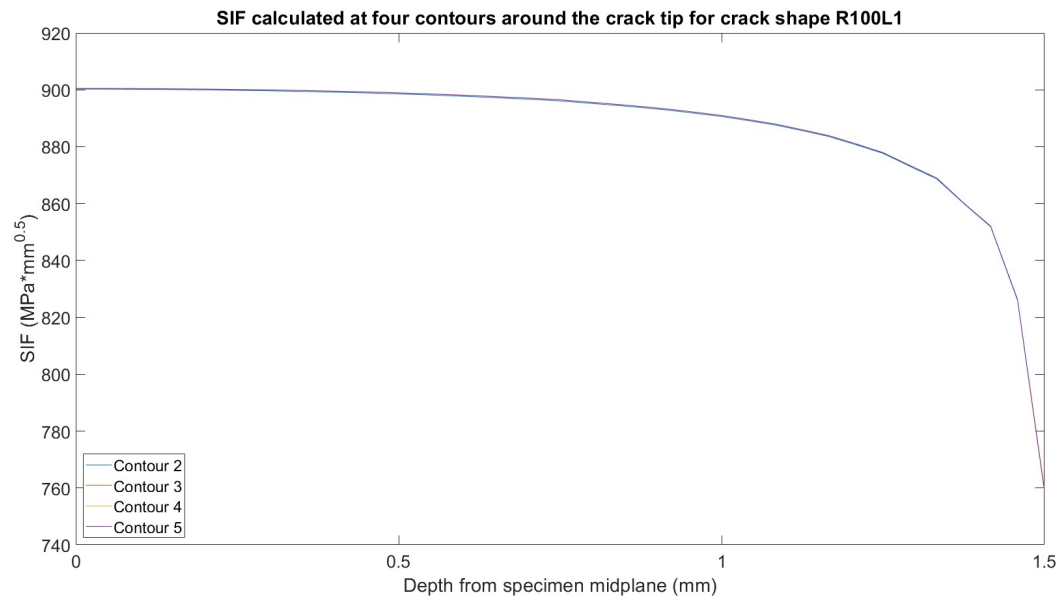


$$\text{Ratio} = (R-x)/R\theta$$

→ $1/\theta$ at the crack

Inherent meshing difficulties

- 5 contours seems to be enough to enable SIF result convergence

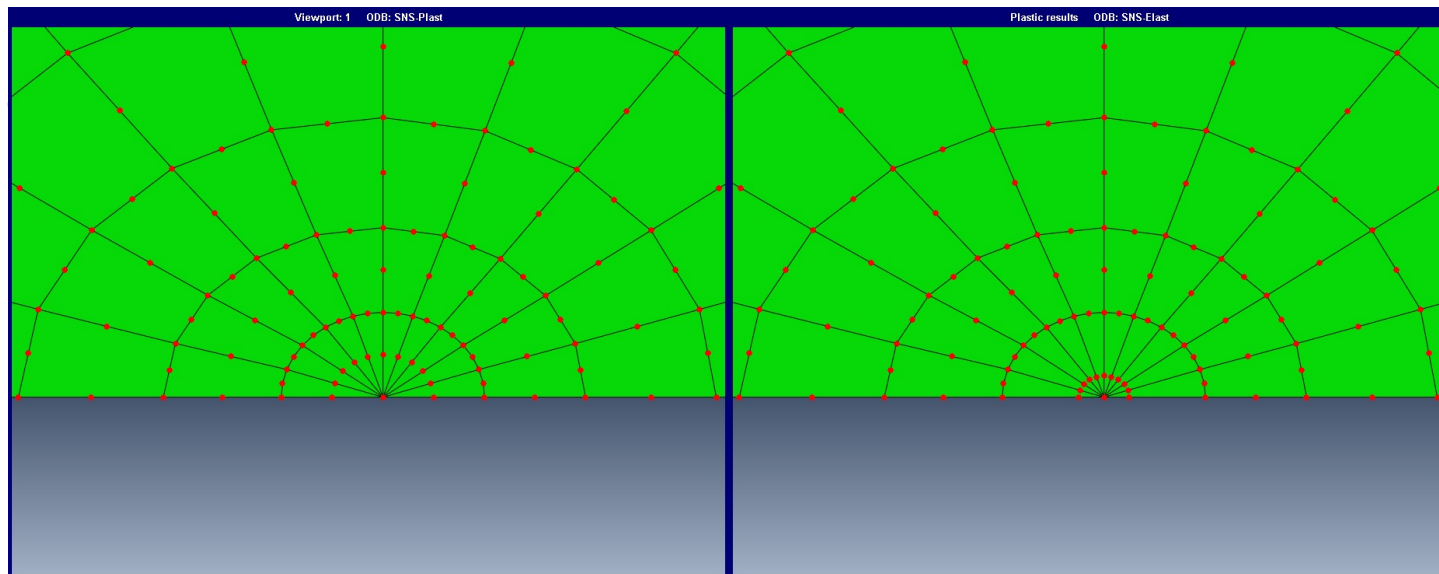


Inherent meshing difficulties

- Cylindrical load introduction sections are geometrically complex
- Tetragonal elements can't be used around the crack tip
 - Two separate meshes and a tie constraint

Inherent meshing difficulties

- Crack singularity must be taken into account:
 - Inverse singularity for plastic model, duplicate midside nodes



Elastic analysis

- Issues in field importation

- Abaqus can only import fields at nodes, resulting in two consecutive interpolations when mapping integration point fields

```

935 f = elastModel.MappedField(name='SDV Field',
936   description='', regionType=MESH, partLevelData=False, localCsys=None,
937   mappingAlgorithm=VOLUMETRIC, defaultUnMappedValue=100.0)
938
939
940 f.OdbMeshRegionData(odbFileName=odbName,
941   variableLabel='SDV2', stepIndex=1, frameIndex=1,
942   quantityToPlot=FIELD_OUTPUT, averageElementOutput=False,
943   useRegionBoundaries=True, regionBoundaries=ODB_REGIONS,
944   includeFeatureBoundaries=True, averageOnlyDisplayed=False,
945   computeOrder=EXTRAPOLATE_COMPUTE_AVERAGE, averagingThreshold=100.0,
946   numericForm=REAL, complexAngle=0.0, featureAngle=20.0, dataType=SCALAR,
947   displayDataType=SCALAR, outputPosition=INTEGRATION_POINT,
948   displayOutputPosition=NODAL, refinementType=NO_REFINEMENT,
949   refinementLabel='', refinementIndex=-1, sectionPoint=())
950
951
952
953 elastModel.Field(name='SDV Field Predefined',
954   createStepName='Initial', region=elastModel.rootAssembly.instances['crackedBlock-1'].sets['Block - Plastic Zone'],
955   distributionType=FIELD, crossSectionDistribution=CONSTANT_THROUGH_THICKNESS,
956   field='SDV Field', fieldVariableNum=1, magnitudes=(1.0, ))
957

```



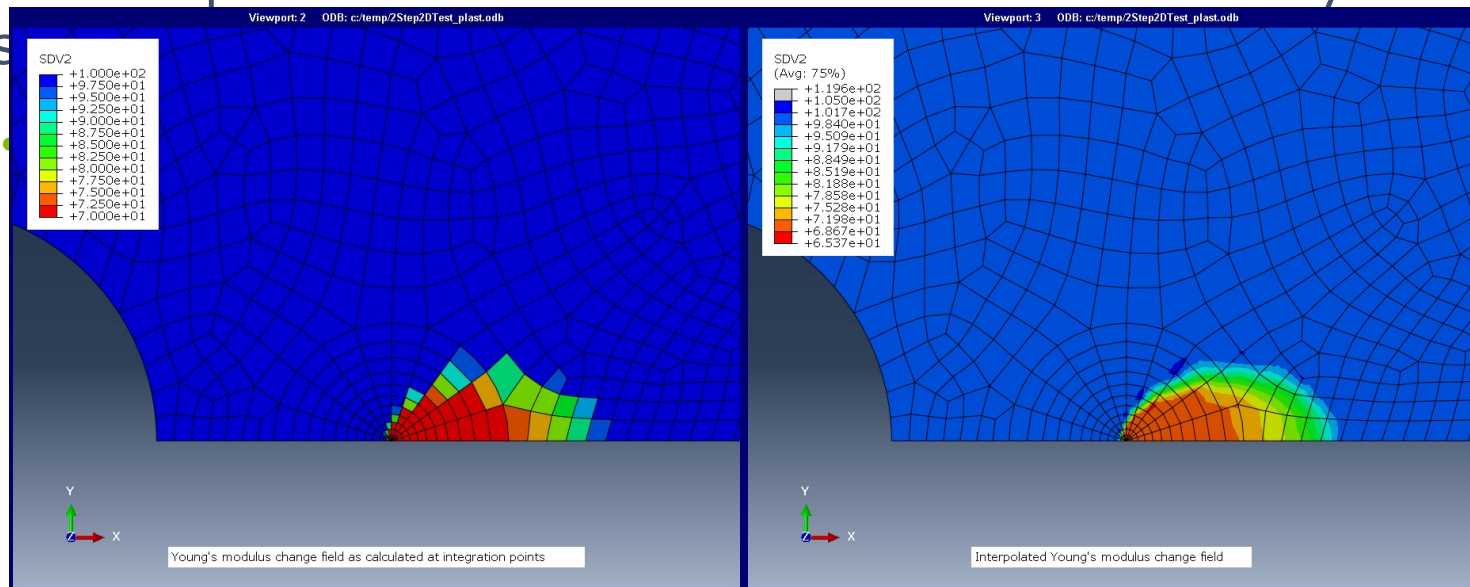
```

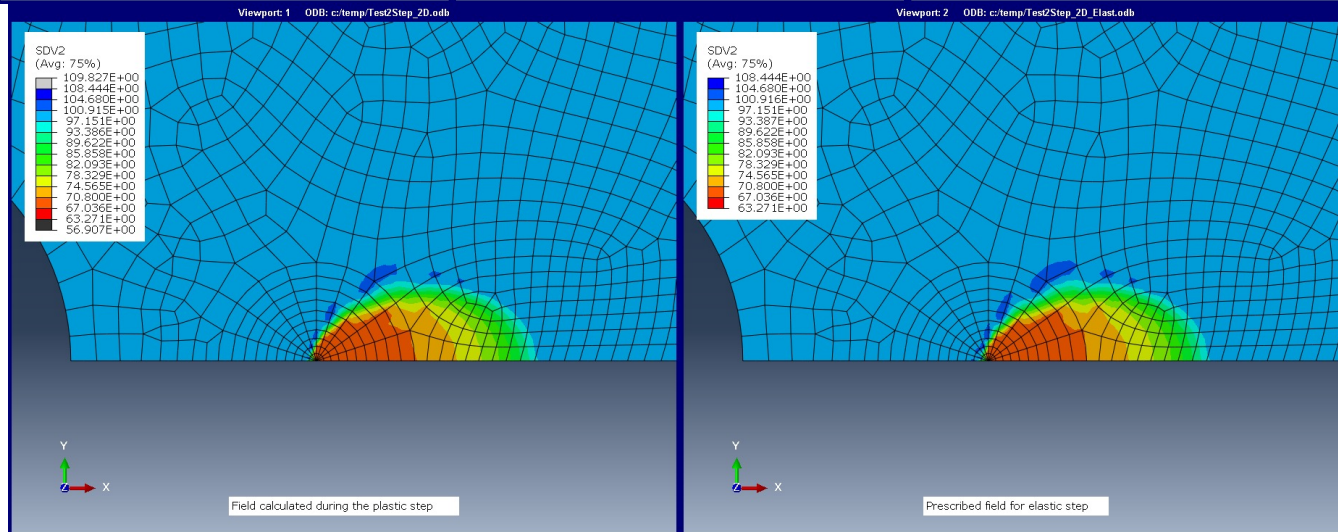
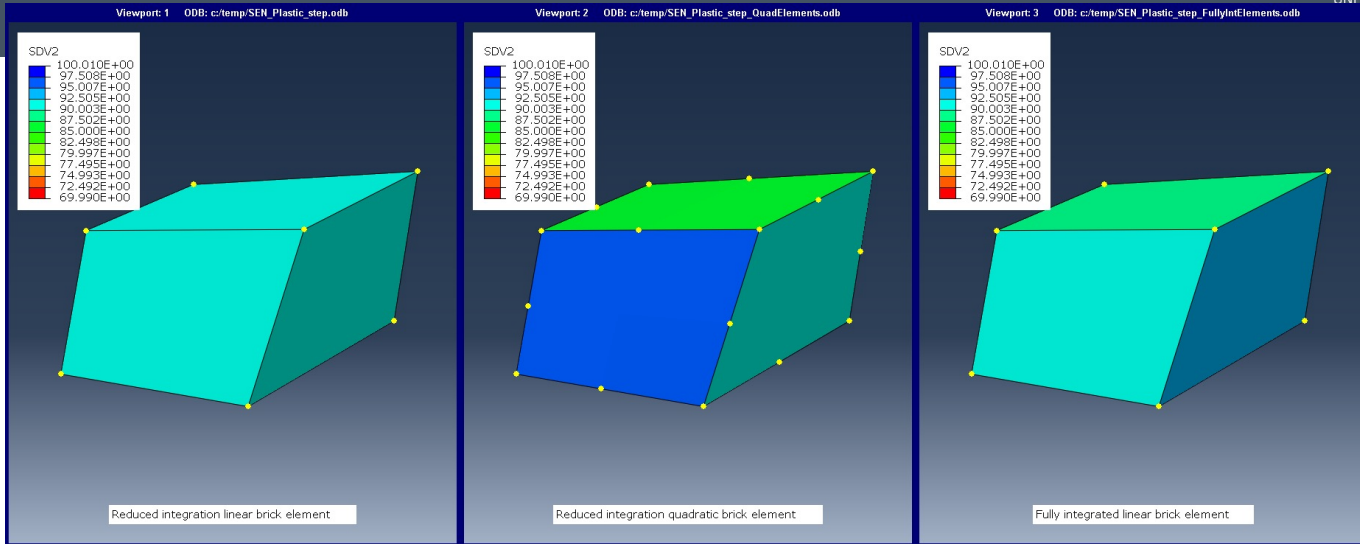
458611 *Elastic, dependencies=1
458612 223120., 0.3, , 82.332
458613 271000., 0.3, , 100.
458614 *User Defined Field
458615 **
458616 ** FREDEFINED FIELDS
458617 **
458618 ** Name: SDV Field Predefined Type: Field Using Field: SDV Field
458619 *Initial Conditions, type=FIELD, variable=1
458620 crackedBlock-1.1, 99.3858
458621 crackedBlock-1.2, 99.9997
458622 crackedBlock-1.3, 100.003
458623 crackedBlock-1.4, 90.8995
458624 crackedBlock-1.5, 99.9997
458625 crackedBlock-1.6, 99.9676
458626 crackedBlock-1.7, 91.1936
458627 crackedBlock-1.8, 99.4275
458628 crackedBlock-1.9, 100.
458629 crackedBlock-1.10, 100.
458630 crackedBlock-1.11, 100.
458631 crackedBlock-1.12, 100.
458632 crackedBlock-1.13, 100.
458633 crackedBlock-1.14, 100.
458634 crackedBlock-1.15, 100.
458635 crackedBlock-1.16, 100.
458636 crackedBlock-1.17, 100.
458637 crackedBlock-1.18, 100.
458638 crackedBlock-1.19, 100.
458639 crackedBlock-1.20, 100.
458640 crackedBlock-1.21, 99.9997
458641 crackedBlock-1.22, 100.
458642 crackedBlock-1.27, 97.1686
458643 crackedBlock-1.28, 97.471
458644 crackedBlock-1.29, 100.
458645 crackedBlock-1.30, 99.9997
458646 crackedBlock-1.31, 100.
458647 crackedBlock-1.32, 100.
458648 crackedBlock-1.33, 100.
458649 crackedBlock-1.34, 99.9997
458650 crackedBlock-1.35, 100.
458651 crackedBlock-1.36, 100.

```

Issues in field importation

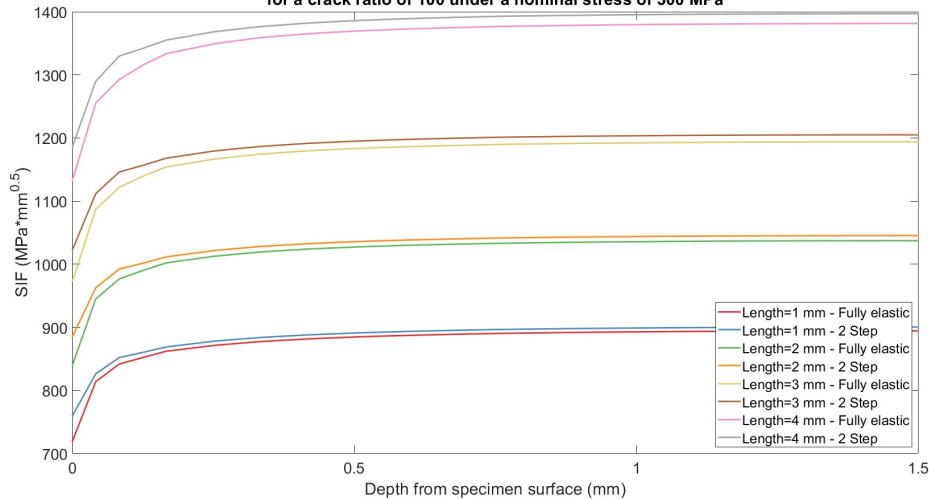
- Neither point cloud or mesh-to-mesh method truly



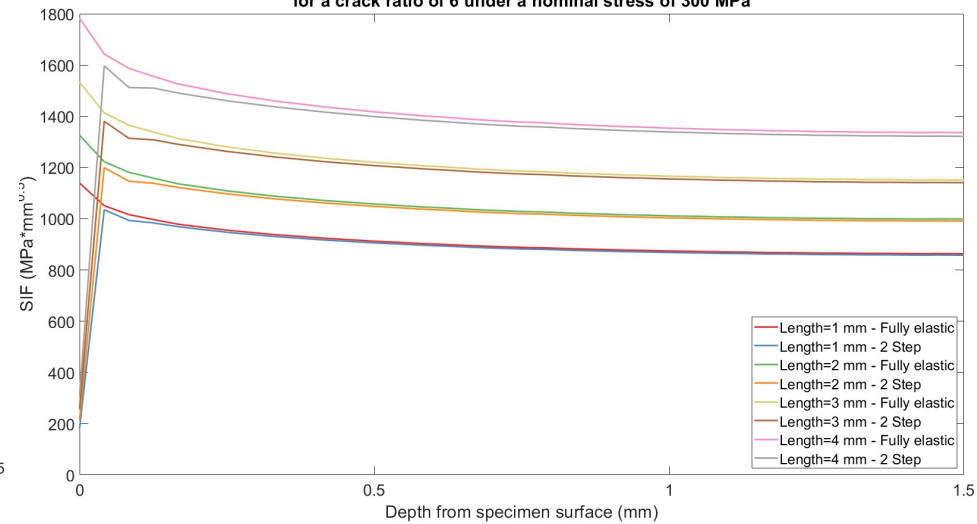


Low stress state : 300 MPa for 1mm pre-crack

SIF calculated for four crack lengths and both material models for a crack ratio of 100 under a nominal stress of 300 MPa



SIF calculated for four crack lengths and both material models for a crack ratio of 6 under a nominal stress of 300 MPa



Low stress state : 300 MPa for 1mm precrack (continued)

